

ANGLE OF ATTACK AND WHEEL-RAIL WEAR



FINAL REPORT

~~DEC 1981~~

June 1982

Document is available to the public through the
National Technical Information Service,
Springfield, Virginia 22161.

Prepared for

**U.S. DEPARTMENT OF TRANSPORTATION
FEDERAL RAILROAD ADMINISTRATION
Office of Research and Development
Washington, D.C. 20590**

| | | | | | |
|---|--|--|--|--|-----------|
| 1. Report No. | | 2. Government Accession No. | | 3. Recipient's Catalog No. | |
| 4. Title and Subtitle ANGLE OF ATTACK AND WHEEL-RAIL WEAR | | | | 5. Report Date Dec. 1981. | |
| | | | | 6. Performing Organization Code | |
| | | | | 8. Performing Organization Report No. IIT-TRANS-81-2 | |
| 7. Author(s) Dr.S.Kumar, D.L.Prasanna Rao, B.R.Rajkumar | | | | 10. Work Unit No. (TRAIS) | |
| 9. Performing Organization Name and Address Illinois Institute of Technology. (IIT) 3300 S. Federal St. Chicago, IL-60616. | | | | 11. Contract or Grant No. DOT-FR-744-4301 | |
| | | | | 13. Type of Report and Period Covered Technical Report(Final) (June-Dec. 1980) | |
| | | | | 14. Sponsoring Agency Code | |
| 12. Sponsoring Agency Name and Address Federal Railroad Administration. (FRA) Office of Research and Development 400 7th Street, SW Washington, D.C. 20590 | | | | | |
| 15. Supplementary Notes Investigation conducted in cooperation with The Griffin Wheel Co. and The General Motors (EMD). | | | | | |
| 16. Abstract Angle of attack is one of the most important parameters influencing wheel and rail wear. Some experiments conducted on the IIT-GMEMD 1/4.5 test facility to study wear of wheels and rails are reported. The angle of attack range covered is from $\theta=0.25^\circ$ to $\theta=1.00^\circ$. The drastic reduction in wheel and rail life at high angles of attack is highlighted by comparison of the test results at 0.25° and 0.76° angle of attack. The adhesion-creepage behavior of wheel-rail contact in the longitudinal and lateral directions is examined and shown to be qualitatively similar for the two directions. Validity of the flange wear indices, obtained by the friction center method and those proposed by CN and Ghonem and Kalousek, are checked against the wear rates obtained in laboratory experiments. It is concluded that none of the indices allows for the effect of all the parameters. The index proposed by Marcotte, Caldwell and List appears to have reasonably good agreement with the limited experimental data generated here. Further experimental investigation is needed to establish the relevance and validity of wear indices as applicable to wheel/rail wear. | | | | | |
| 17. Key Words Wear, Wear index, Wear rate, Rail/wheel, Adhesion, Creepage, Flange force, Flange wear. | | | 18. Distribution Statement Document is available through the National Technical Information Service, 5285 Port Royal Road, Springfield, VA. 22161 | | |
| 19. Security Classif. (of this report) Unclassified | | 20. Security Classif. (of this page) Unclassified | | 21. No. of Pages | 22. Price |

TABLE OF CONTENTS

| | <u>Page No</u> |
|---|----------------|
| 1. INTRODUCTION | 1 |
| 2. PRESENT INVESTIGATION | 2 |
| 3. FRICTION-CREEPAGE RELATION | 3 |
| 4. WEAR RATES OF WHEEL AND RAIL-INFLUENCE OF ANGLE OF ATTACK | 7 |
| 5. FLANGE WEAR INDICES AND FLANGE WEAR RATES | 28 |
| 6. CONCLUDING REMARKS | 36 |
| 7. RECOMMENDATIONS FOR FUTURE WORK | 38 |
| 8. REFERENCES | 40 |

LIST OF FIGURES

| <u>FIGURE</u> | | <u>PAGE</u> |
|---------------|--|-------------|
| 1 | μ vs. ξ for 100T Car Geom. Simulation | 4 |
| 2 | μ vs. ξ (Longitudinal) for 100T Car | 4 |
| 3 | Microphotograph of Wheel at 6750 cyc. ($\theta=0.76$) | 8 |
| 4 | Microphotograph of Rail at 5000 cyc. | 9 |
| 5 | Typical Model Wheel Profiles (Talysurf) | 11 |
| 6 | Rail Surface Castings for Surface Analysis | 12 |
| 7 | Rail Profiles by Shadowgraphy | 13 |
| 8 | Wheel Profiles by Shadowgraphy | 14 |
| 9 | Total Wheel Wear Cross Section Area vs. Cycles | 20 |
| 10 | Total Rail Wear Cross Section Area vs. Cycles | 20 |
| 11 | Total Rail and Wheel Wear Cross Section Areas vs. Cycles $\theta = 0.25$ | 21 |
| 12 | Total Rail and Wheel Wear Cross Section Areas vs. Cycles $\theta = 0.76$ | 21 |
| 13 | Wheel Wear Rate vs. Cycles of Loading | 22 |
| 14 | Rail Wear Rate vs. Cycles of Loading | 23 |
| 15 | Wear Rate vs. θ for Wheel and Rail | 24 |
| 16 | W_1 and Flange Wear Rate vs. θ | 30 |
| 17 | W_2 , W_4 , and Flange Wear Rate vs. Cycles | 34 |

1. INTRODUCTION

In an earlier study carried out at IIT, a methodology was proposed for predicting field wear rates based on some data obtained with the IIT-GMEMD Wheel-Rail Simulation Facility at IIT[1]*. The present report represents some further work in the area dealing specifically with the question of the influence of angle-of-attack on the wear of wheels and rails for a 100-ton freight car. Earlier investigations have indicated that the angle-of-attack is probably the single most important parameter contributing to the high rates of wear of both rails and wheels. Since the angle of attack leads to lateral forces in the contact area, the resulting flanging under rolling conditions leads to predominantly gage side and flange wear. It has been established earlier that wear of gage/flange due to angle of attack is more significant than that of the crown/tread due to traction[2]. Hence, the wear studies under angle of attack conditions are performed to be conducted under more realistic geometrical simulation rather than the Hertzian simulation conditions.

Earlier work indicated a non-linear dependence of wear rates on the angle of attack and further established a correlation between the wear rates and some indices of wear suggested by other researchers. However, it may be stated that the question of wear indices and their acceptability needs to be investigated further in order to establish their validity. Such an effort would be of immense help in the wear prediction process.

The foregoing brief comments indicate a need for an investigation which would permit establishing the specific influence of the angle of attack on the wear of wheels and rails. The rest of the report deals with such an effort carried out at the IIT Railroad Laboratory under simulated scaled down experimental conditions. Due to limited fund availability, systematic tests were conducted only for two angles of attack. Using some other earlier limited data, some projections of trends have been attempted. Due to the limited data base, however, this study should be viewed only as an attempt to highlight the various aspects of the problem and to establish a preliminary formulation of the wear versus angle-of-attack relation. Following a brief description of the overall investigation, in Section 2, specific experimental and analytical aspects will be discussed in the rest of the sections of this report.

*Numbers in this kind of paranthesis denote references given in the end of the report.

2. PRESENT INVESTIGATION

The main aim of the present investigation is twofold:
(a) to investigate the relation between angle-of-attack and wheel/rail wear rates for non-tractive contact conditions, and
(b) to check the validity of certain wear indices which have been suggested in the literature.

Tests have been conducted on the IIT-GMEMD facility under the following simulated conditions:

- i) Vertical load on the wheel corresponding to a 100 ton freight car. (Lab load 1302 lbs.)
- ii) An external lateral load corresponding to 1/10 of the vertical load. (130 lbs.)
- iii) Wheel hardness maintained substantially constant for all the tests.
- iv) Standard rail 132 RE geometrical simulation.
- v) Angle of attack values of 0.25° and 0.76° .

The details of the test facility and experimental procedures may be obtained from earlier reports submitted to FRA^[3].

The primary measurements are:

- i) Surface condition established using roughness measurements and micro-photographs.
- ii) Wear cross sectional areas for the wheel and rail separated into tread/flange and crown/gage side wear.
- iii) Flange angles obtained from analysis of castings using a shadowgraph technique.
- iv) Contact area sizes, shapes and relative location using replicating tapes.

3. ADHESION-CREEPAGE RELATION

One of the important parameters, in the conduct of the wear experiments, is the level of adhesion (longitudinal and lateral) during a test. Adhesion, creepage and wear are closely related parameters for wheel and rail performance. The usually accepted definitions of adhesion and creepage are:

$$\begin{aligned} \mu & - \text{Coefficient of adhesion} \\ & = \frac{\text{Tangential force in contact area}}{\text{Normal load in contact area}} \end{aligned}$$

$$\begin{aligned} \xi & - \text{Creepage} \\ & = \frac{\text{Relative slip velocity}}{\text{Pure rolling velocity}} \end{aligned}$$

$$\xi \% = (\xi \times 100).$$

The following subscripts have been used in the text.

- lat - lateral direction
- long - longitudinal direction
- Ext - External

The present series of tests are conducted basically under no traction conditions. But the lateral forces sustained by the contact (crown) and the flange side are defined by the sum of the externally applied lateral loads and the lateral forces generated in the contact due to angle-of-attack. It is very difficult to measure, for a standard wheel, the flange force due to angle-of-attack under flanging conditions. Hence, the adhesion-creepage (μ vs ξ) relation for the longitudinal and lateral directions are established in a separate controlled test when flanging of the test wheel is just prevented in a geometrical simulation trial with angle-of-attack. Under this condition the lateral forces in the contact due to angle-of-attack is sensed by the load cell supporting the wheel. The μ vs ξ relation obtained in such a test for the lateral and longitudinal directions are shown in Figures 1 and 2. Experimental values are shown in Tables 1 and 2. For the lateral direction, the creepage (ξ) is equal to the angle-of-attack in radians. The actual forces sustained by the contact are estimated from these curves in the process of checking out the wear indices.

It is to be noted that the peak values of μ in Figures 1 and 2 correspond to the limiting coefficient μ_c for the two directions. As has been established earlier, the friction coefficient peaks at a certain creepage which is about 1% for a good clean surface and, thereafter, remains substantially constant till a high level of creepage is reached. The downward slope of the

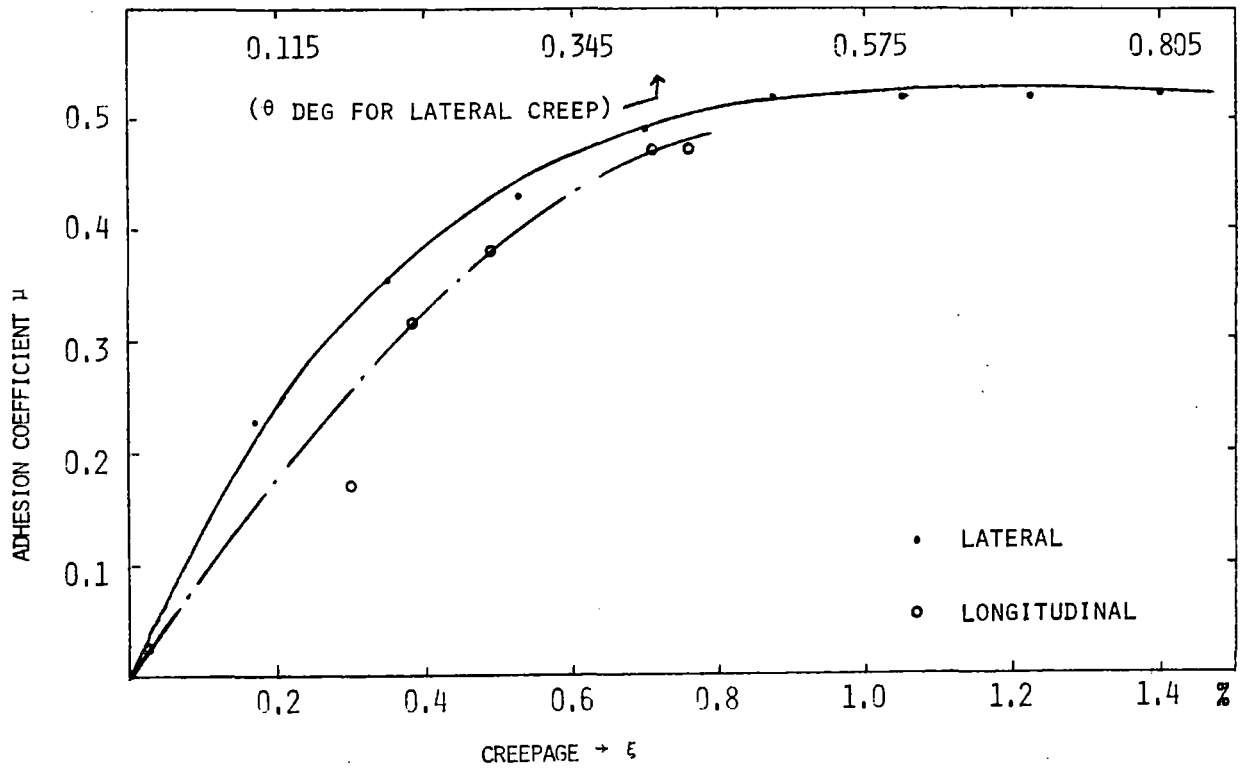


FIG. 1 μ VS ϵ FOR 100T CAR GEOM. SIM.

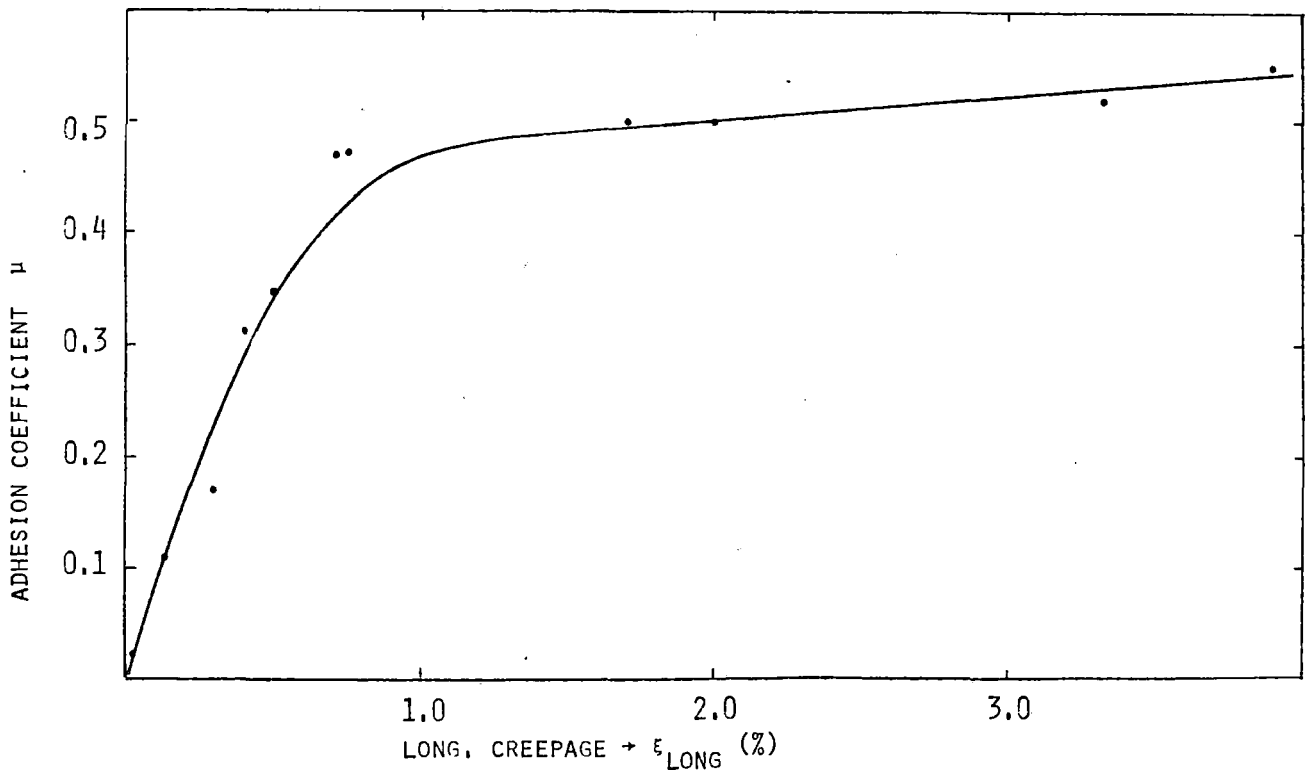


FIG. 2 μ VS ϵ (LONGITUDINAL) 100T CAR GEOM. SIM.

μ vs ξ curve appears to occur at some point in the range of 4% to 15% creepage depending on other parameters which govern the contact mechanics. The μ vs ξ plots also show that the relation is qualitatively the same for the two directions.

TABLE I

μ vs ξ for the longitudinal direction

Geometrical Simulation. Wheel load = 1302 lbs.

| Coefficient of Adhesion μ | Longitudinal Creepage ξ % |
|----------------------------------|----------------------------------|
| 0.005 | 0 |
| 0.028 | 0.027 |
| 0.171 | 0.296 |
| 0.315 | 0.385 |
| 0.378 | 0.488 |
| 0.470 | 0.713 |
| 0.471 | 0.758 |
| 0.500 | 1.722 |
| 0.552 | 3.915 |

TABLE 2

μ vs ξ for the lateral direction

Geometrical simulation, 100T car

Wheel load = 1302 lbs.

| θ (deg) | ξ_{lat} (%) | ξ_{long} (%) | $\mu_{lateral}$ |
|----------------|-----------------|------------------|-----------------|
| 0.1 | 0.175 | 0.07 | 0.225 |
| 0.2 | 0.349 | 0.03 | 0.353 |
| 0.3 | 0.524 | 0.05 | 0.429 |
| 0.4 | 0.696 | 0.04 | 0.491 |
| 0.5 | 0.872 | 0.04 | 0.522 |
| 0.6 | 1.047 | 0.04 | 0.521 |
| 0.7 | 1.222 | 0.02 | 0.517 |
| 0.8 | 1.396 | 0.02 | 0.524 |
| 0.9 | 1.570 | 0.00 | 0.466 |
| 1.0 | 1.745 | 0.02 | 0.468 |

4. WEAR RATES OF WHEEL AND RAIL - INFLUENCE OF ANGLE OF ATTACK

As has been stated earlier, the present investigation is an effort to highlight the influence of angle of attack in the wear process of wheels and rails. The other parameters which are of significance in the process are held constant. Results from a series of tests at 0.25° and 0.76° angle-of-attack will be presented together with some limited data obtained in an earlier experiment at 0.5° attack. The test conditions are:

- i) 1:4.5 scale simulation of rail and wheel.
- ii) Simulation of a non tractive wheel of a 100 ton car. Total simulation of wheel-rail geometry (geometrical simulation) and contact stress conditions. Laboratory wheel normal load = 1302 lbs.
- iii) Angles of attack of 0.25° and 0.76° for two series of tests.
- iv) In addition to flange loading due to angle of attack, an external lateral load of approximately 130-150 lbs. is maintained on the small wheel.
- v) The coefficient of adhesion in the longitudinal direction was maintained at a very low level (< 0.075) during the entire test in order to simulate the non traction/braking condition. The corresponding longitudinal creepage is of the order of 0.02 %, which is close enough to zero creep condition.
- vi) Individual test duration determined by the flange wear region extending close to the flange top.
- vii) Rail Hardness = 31 Shore
Wheel Hardness = 33-34 Shore
Big Wheel (Rail) Dia. = 36.365"
Small Wheel (Wheel) Dia. = 8.031"

The main measurements during the test are:

a) During each test, the contact conditions are established through tape impressions. This provides an estimate of the changing contact shapes, both tread and flange, and can be used to estimate the average contact stresses, distance between flange and tread contact points, etc. Further details of this aspect will however not be included in the present report.

b) The surface condition is assessed through the micro-photographs with magnification in the range x10 to x20. Some typical photographs are shown in Figures 3 and 4.



(a)

(a) FLANGE



(b)

(b) TREAD

FIG. 3 MICROPHOTOGRAPH OF WHEEL AT 6750 CYC. ($\theta = 0.76$ DEG.)



FIG. 4 MICROPHOTOGRAPH OF RAIL.

5000 cyc.
 $\theta = 0.76$ DEG.
(X10)

c) The loads in the contact region in the various directions are monitored during the entire test using a strain gage load cell and associated instrumentation. Some test results are tabulated in Table 3.

d) The speeds of the two wheels are monitored during the test through the use of two optical shaft encoders mounted on the two shafts. These provide 1000 pulses per revolution of the wheel and using a typical sampling time of 1 second, it is possible to obtain the longitudinal creepage in the contact zone defined in the relation

$$\text{longitudinal creepage } (\xi\%) = \left[1 - \frac{D_2 n_2}{D_1 n_1} \right] \times 100\%$$

where D_1 and D_2 are the diameters of the wheels representing the rail and wheel² in the simulation and n_1 and n_2 are pulse counts of the two wheels during a sampling period.

e) The most important measurement carried out during a test is that of the wear cross section areas. For this purpose, an acrylic casting is obtained of the rail and wheel surface at initial time and at regular intervals during the test. The casting provides an accurate replica of the surface and can be used for studying the surface profiles as also the surface roughness. Reference lines and surfaces on the rail and wheel, outside the zone of influence of plastic flow and wear, are used in the process of matching castings to obtain wear cross section areas. The fact that certain parts of the rail and wheel are not subject to either plastic flow or wear due to the contact conditions aids immensely in the process of using the casting technique. Once the castings are obtained, the profile analysis may be carried out by one of two methods.

In the first method, the casting surface is analyzed using a Talysurf -10 profilometer. By limiting the magnification to 10, one is able to obtain a plot of the entire profile of both the wheel and rail. Comparison of the castings at any stage of the test with the initial casting provides an estimate of the wear and plastic flow areas. Typical Talysurf plots are shown in Figure 5.

A second method of casting analysis, which has been tried out for the first time in the present series of tests, consists of using a shadowgraph in conjunction with thin slices of the castings which are obtained following machining. The castings can be machined using band saws for cutting and grinding wheels for finishing the surfaces for viewing. Figure 6 shows the casting prepared for Talysurf analysis and for shadowgraphy. The shadowgraph permits viewing the entire profile with magnifications up to 20 with the result that the initial profile and worn profiles can be drawn superimposed. The profiles of the wheel and rail during the test with $\theta = 0.75^\circ$ are shown in Figures 7 and 8.

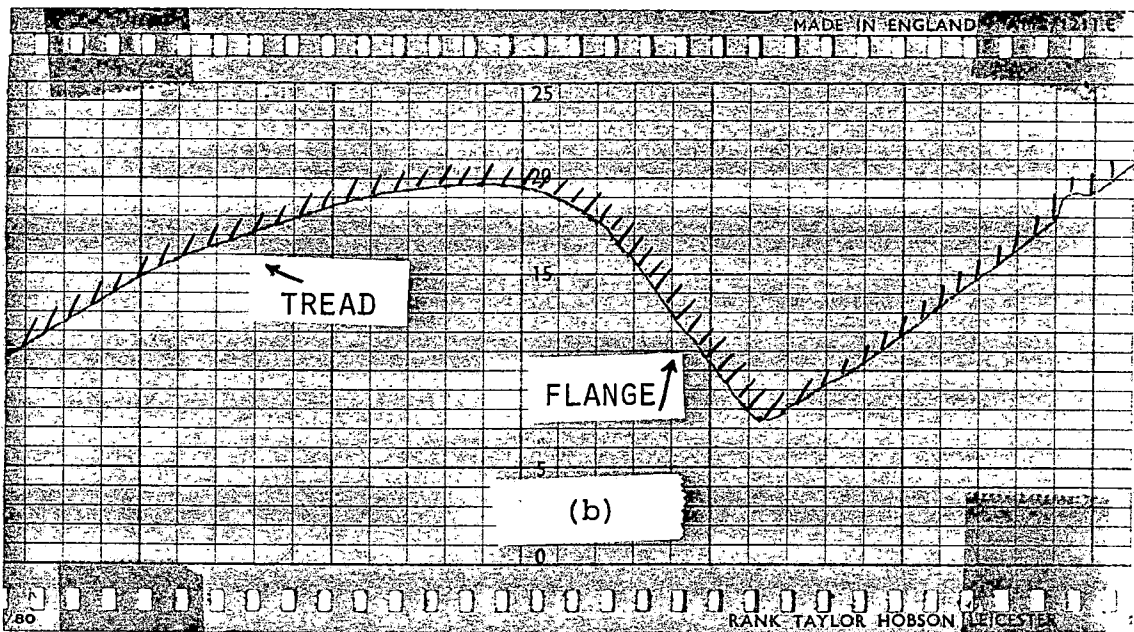
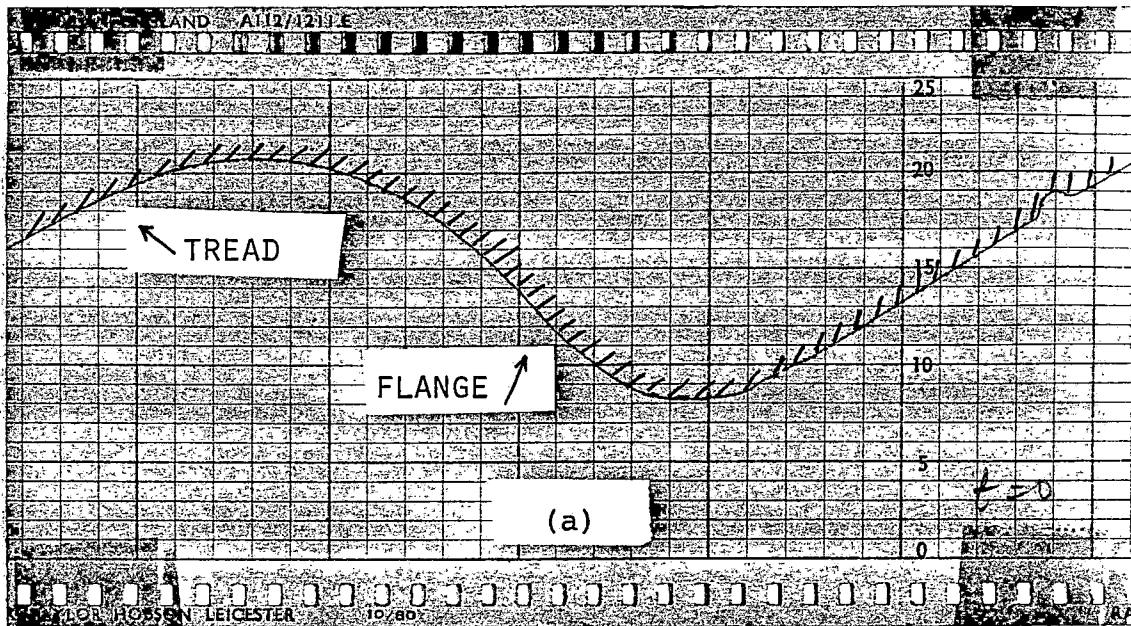
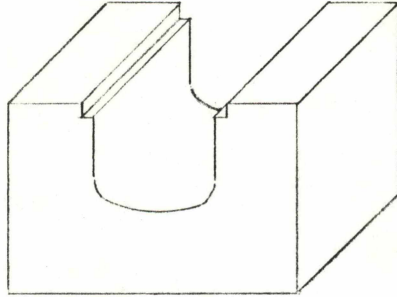


FIG. 5 TYPICAL MODEL WHEEL PROFILES (TALYSURF)

$\theta = 0.76$ DEG.

MAG X10

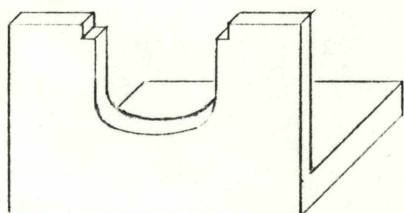
(a) INITIAL (b) FINAL.
(NEW) (WORN)



CASTING FOR TALYSURF ANALYSIS

- i) Profile
- ii) Surface roughness

FIG. 6 RAIL SURFACE CASTINGS



CASTING FOR SHADOWGRAPHY

(Thin Slice)
i) Profile only

FOR SURFACE ANALYSIS.

TANGENT TO PROFILE AT
18.0 DEG. TO HORIZONTAL,
RAIL= MAG X20,
WEAR TEST, $\theta=0.76$ DE
REF=REFERENCE

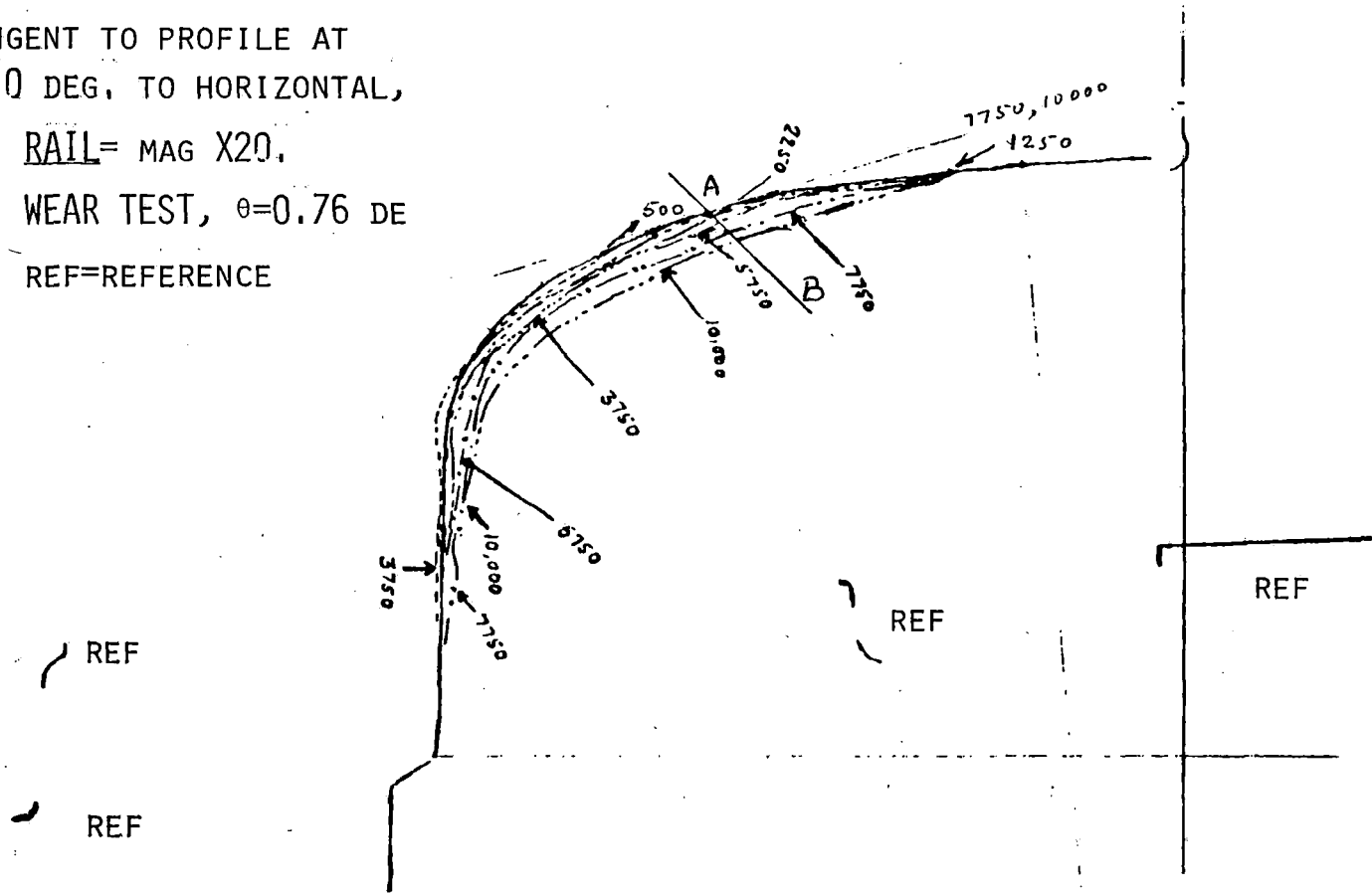


FIG. 7 PROFILES BY SHADOWGRAPHY (RAIL).

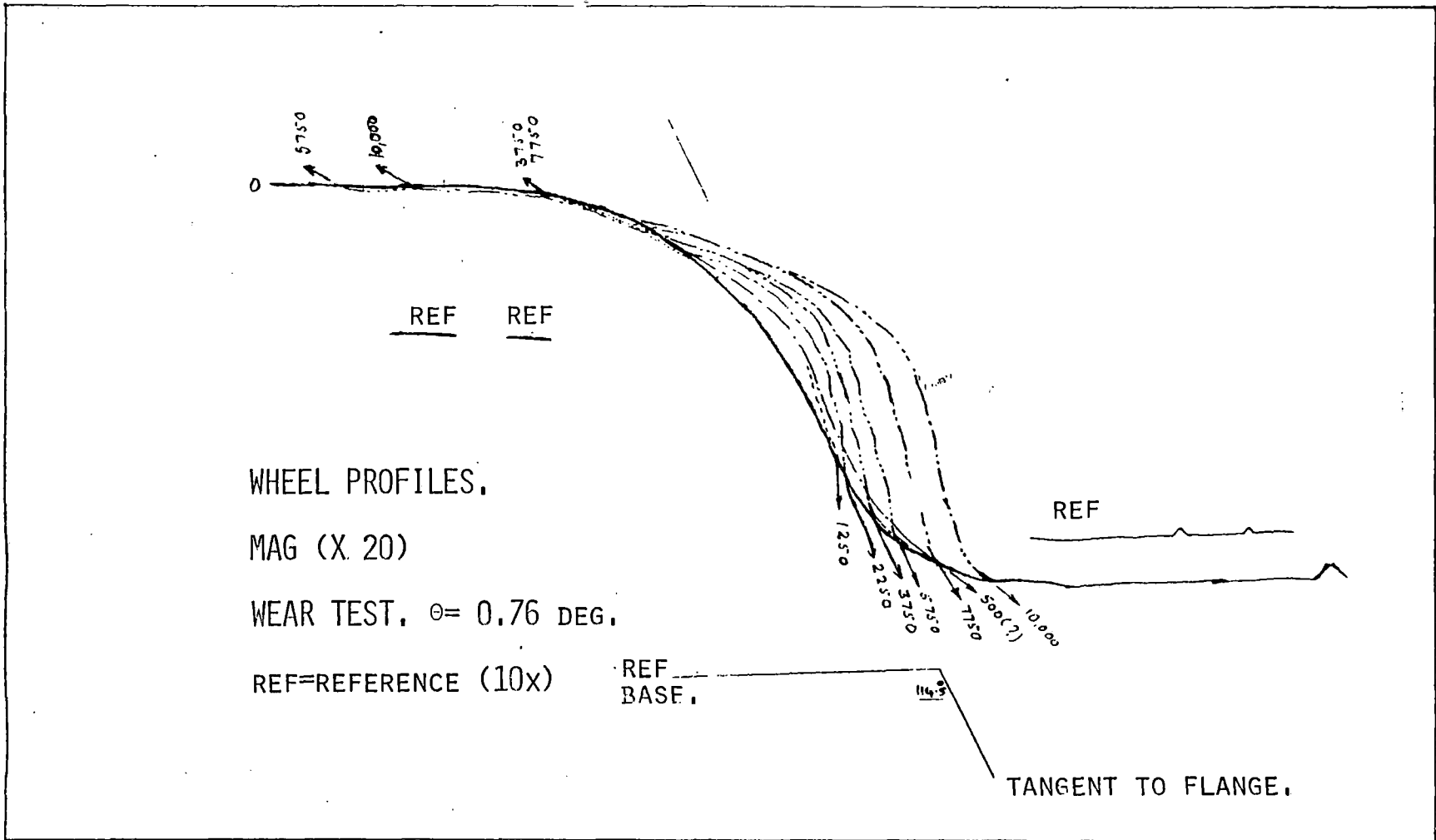


FIG. 8 WHEEL PROFILES BY SHADOWGRAPHY.

TABLE 3

Monitored contact load data

Wear test $\theta = 0.76^\circ$

| NO. | TEST RANGE (big wheel cyc.) | LOAD (lbs) | | | Lat. external |
|-----|--------------------------------|------------|-------|------|------------------|
| | | Vertical | Long. | Lat. | |
| 1 | 0-100 | 1296 | 53 | 182 | 161 |
| 2 | 100-500 | 1229 | 86 | 176 | 157 |
| 3 | 500-1250 | 1248 | 87 | 163 | 152 |
| 4 | 1250-2250 | 1255 | 52 | 162 | 150 |
| 5 | 2250-3750 | 1166 | 84 | 163 | 150 |
| 6 | 3750-4250 | 1322 | 80 | 181 | 155 |
| 7 | 4250-4500 | 1281 | 93 | 176 | 154 |
| 8 | 4500-5000 | 1303 | 81 | 169 | 151 |
| 9 | 5000-5750 | 1289 | 98 | 171 | 151 |
| 10 | 5750-6750 | 1289 | 87 | 175 | 151 |
| 11 | 6750-7750 | 1322 | 76 | 173 | 151 |
| 12 | 7750-10,000 | 1292 | 78 | 172 | 148 |

Figures 9 and 10 show the wheel and rail wear cross sectional areas vs. loading cycles for the various values of the angle of attack on a semi log plot. The curves show the increasing wear rate as the test proceeds. Crown and gage side wear of a rail can be readily defined in terms of a point of demarcation on the rail where the flange forces (lateral) assume importance. In measuring the wear cross section areas, the division of the total wear area into flange and tread wear is carried out by the following method. Point A (Fig. 7) is defined by the tangent at an approximate angle of 18° to the tangent at the rail top. This point which is in fact close to the mid point of the first transition radius on the rail has been arrived at after considerations of the initial tread and flange contact areas and their growth during the test. Line AB drawn at 45° to the horizontal is then used for dividing the wear area into flange and tread wear. For the wheel, a point corresponding to point A on the rail is established by profile matching and the procedure, as laid down for the rail, is repeated.

In all the tests one can notice a trend towards a stabilization of the wear rate indicated by the total wear vs. loading cycle plots. The significant effect of the angle of attack is brought out by the fact that comparable wear occurs for the $\theta = 0.76^\circ$ test at 10,000 cycles and for the $\theta = 0.25^\circ$ test at 100,000 cycles. The wear data is shown tabulated in Table 4 (a), (b) and (c) for purposes of estimating the wear rates. The wear areas are shown plotted in Figs. 11 and 12 also.

For the purpose of obtaining the wear rates for the wheel and rail, a regression analysis was carried out with polynomials being fitted to the data. The main features of the fit such as the error of fit at initial time and standard deviation of the fit are shown in Table 5 (a) and (b). The wear rate vs. cycles of loading relation is shown tabulated in Table 6 (a) and (b). Use of this method however calls for considerable care as the choice of the order of fit cannot be based entirely on the value of the standard deviation alone, since low standard deviations of the higher order of polynomials are also associated with noticeably less smoothening of the data points.

For the purpose of the present study, the wear rates have been estimated at load cycles corresponding to 20%, 50% and 100% of the total test duration for the $\theta = 0.25^\circ$ and $\theta = 0.76^\circ$ curves from Fig. 9 through 12. The values are tabulated in Table 7 and plotted in Figs. 13, 14 and 15. It is to be noted that in presenting Fig. 15, it is implied that similar stages in the tests are being compared. For example the total test durations are 100,000 cycles (approx) at 0.25° angle-of-attack, and 10,000 cycles at 0.76° angle-of-attack. Thus the 20% test points in Fig. 15 corresponds to 2000 cycles. For the 0.76° test and 20,000 cycles for the 0.25° test.

The differences between columns 1 and 2, for the wear rates, listed in Table 7 are due to the fact that Fig. 9 and 10 are semi-

TABLE 4(a) WEAR DATA $\theta=0.25^\circ$

Wear cross section in 10^{-4}in^2 units

| CYCLES | RAIL | | | WHEEL | | |
|---------|------|-------|-------|--------|-------|-------|
| | GAGE | CROWN | TOTAL | FLANGE | TREAD | TOTAL |
| 5,500 | 2.1 | -0.4 | 1.7 | 1.5 | 1.1 | 2.6 |
| 12,500 | -0.3 | -1.7 | -2.0 | 5.6 | -5.3 | 0.3 x |
| 26,000 | 1.6 | 3.9 | 5.5 | 10.2 | -3.6 | 6.6 |
| 42,500 | 5.1 | 10.1 | 15.2 | 22.4 | 2.2 | 24.6 |
| 53,500 | 6.3 | 7.65 | 13.95 | 28.5 | 3.3 | 31.8 |
| 73,000 | 11.2 | 11.9 | 23.1 | 39.3 | 8.6 | 47.9 |
| 90,000 | 11.5 | 13.4 | 24.9 | 48.0 | 19.8 | 67.8 |
| 111,000 | 20.3 | 12.5 | 32.8 | 58.6 | 23.4 | 82.0 |

TABLE 4(b) WEAR DATA $\theta=0.5^\circ$

| | | | | | | |
|------|------|------|------|------|------|------|
| 600 | 1.52 | - | 1.52 | 2.30 | 0.35 | 2.45 |
| 1200 | 1.90 | 1.52 | 3.42 | 2.48 | 0.61 | 3.09 |
| 1800 | 3.04 | 2.74 | 5.78 | 2.66 | 0.91 | 3.57 |
| 2400 | 3.80 | 3.04 | 6.84 | 3.62 | 1.17 | 4.79 |

TABLE 5(a)

Departure of wear cross section from zero at initial time

| ORDER OF FIT | $\theta = 0.25$ | | $\theta = 0.5$ | | $\theta = 0.76$ | | | |
|--------------|-----------------|-------|----------------|-------|-----------------|----------|---------|----------|
| | RAIL | WHEEL | RAIL | WHEEL | RAIL(T) | WHEEL(T) | RAIL(S) | WHEEL(S) |
| 1 | -1.46 | -6.46 | -0.05 | 0.42 | -3.44 | -6.94 | -0.81 | -4.12 |
| 2 | -1.7 | -2.76 | -0.09 | 0.17 | -1.42 | -0.96 | 3.12 | 0.64 |
| 3 | -1.14 | 0.17 | 0.07 | 0.007 | 0.19 | 1.05 | 1.33 | -0.08 |
| 4 | 0.44 | 0.74 | | | -0.29 | -0.44 | -0.005 | -0.10 |
| 5 | 0.78 | 1.65 | | | 0.088 | 0.18 | 0.09 | 0.18 |
| 6 | 1.74 | -0.58 | | | | | | |

(T) Talysurf

(S) Shadowgraphy

TABLE 5(b)

Standard deviation of fit

| | | | | | | | | |
|---|------|------|------|-------|------|------|------|------|
| 1 | 2.23 | 4.32 | 0.17 | 0.31 | 3.79 | 5.09 | 3.63 | 3.62 |
| 2 | 2.22 | 3.09 | 0.17 | 0.24 | 1.49 | 2.73 | 2.28 | 1.19 |
| 3 | 2.17 | 1.91 | 0.06 | 0.027 | 1.10 | 2.17 | 1.74 | 1.03 |
| 4 | 1.74 | 1.85 | | | 0.92 | 1.11 | 0.49 | 1.03 |
| 5 | 1.71 | 1.66 | | | 0.38 | 0.95 | 0.45 | 0.83 |
| 6 | 1.79 | 1.15 | | | | | | |

TABLE 6(a)

Wear rate in $10^{-4} \text{ in}^2/1000 \text{ cyc.}$ (Based on polynomial fit)

(1. First order 2. Second order 3. Third order) $\theta = 0.25^\circ$

| CYCLES | RAIL | | | WHEEL | | |
|---------|-------|-------|-------|-------|-------|--------|
| | 1. | 2. | 3. | 1. | 2. | 3. |
| 0 | 0.309 | 0.328 | 0.230 | 0.173 | 0.11 | -0.002 |
| 1000 | 0.309 | 0.328 | 0.234 | 0.173 | 0.11 | 0.004 |
| 3000 | 0.309 | 0.327 | 0.243 | 0.173 | 0.113 | 0.017 |
| 5000 | 0.309 | 0.326 | 0.251 | 0.173 | 0.116 | 0.029 |
| 10,000 | 0.309 | 0.325 | 0.269 | 0.173 | 0.122 | 0.059 |
| 25,000 | 0.309 | 0.319 | 0.312 | 0.173 | 0.14 | 0.134 |
| 50,000 | 0.309 | 0.311 | 0.338 | 0.173 | 0.17 | 0.207 |
| 100,000 | 0.309 | 0.293 | 0.22 | 0.173 | 0.23 | 0.167 |

19

TABLE 6(b)

Wear rate based on polynomial fit ($10^{-4} \text{ in}^2/10^3 \text{ cycles}$)

$\theta = 0.75^\circ$

1, 2, 3 orders of polynomial T=Talysurf S=Shadowgraph

| CYCLES | RAIL | | | | | | WHEEL | | | | | |
|-------------------|------|------|------|------|-------|-------|-------|------|------|------|------|------|
| | 1(T) | 1(S) | 2(T) | 2(S) | 3(T) | 3(S) | 1(T) | 1(S) | 2(T) | 2(S) | 3(T) | 3(S) |
| 0 | 6.01 | 4.06 | 2.33 | 1.08 | 4.49 | 4.23 | 2.39 | 1.99 | 1.38 | 1.19 | 0.59 | 1.47 |
| 1000 | 6.01 | 4.06 | 3.07 | 1.68 | 4.19 | 3.29 | 2.39 | 1.99 | 1.58 | 1.35 | 1.18 | 1.49 |
| 2000 | 6.01 | 4.06 | 3.81 | 2.28 | 4.12 | 2.69 | 2.39 | 1.99 | 1.79 | 1.51 | 1.68 | 1.55 |
| 4000 | 6.01 | 4.06 | 5.29 | 3.47 | 4.68 | 2.53 | 2.39 | 1.99 | 2.19 | 1.83 | 2.42 | 1.75 |
| 6000 | 6.01 | 4.06 | 6.77 | 4.67 | 6.17 | 3.72 | 2.39 | 1.99 | 2.59 | 2.16 | 2.82 | 2.07 |
| 8000 ^r | 6.01 | 4.06 | 8.25 | 5.86 | 8.59 | 6.29 | 2.39 | 1.99 | 3.00 | 2.48 | 2.87 | 2.52 |
| 10,000 | 6.01 | 4.06 | 9.73 | 7.06 | 11.96 | 10.23 | 2.39 | 1.99 | 3.41 | 2.80 | 2.58 | 3.08 |

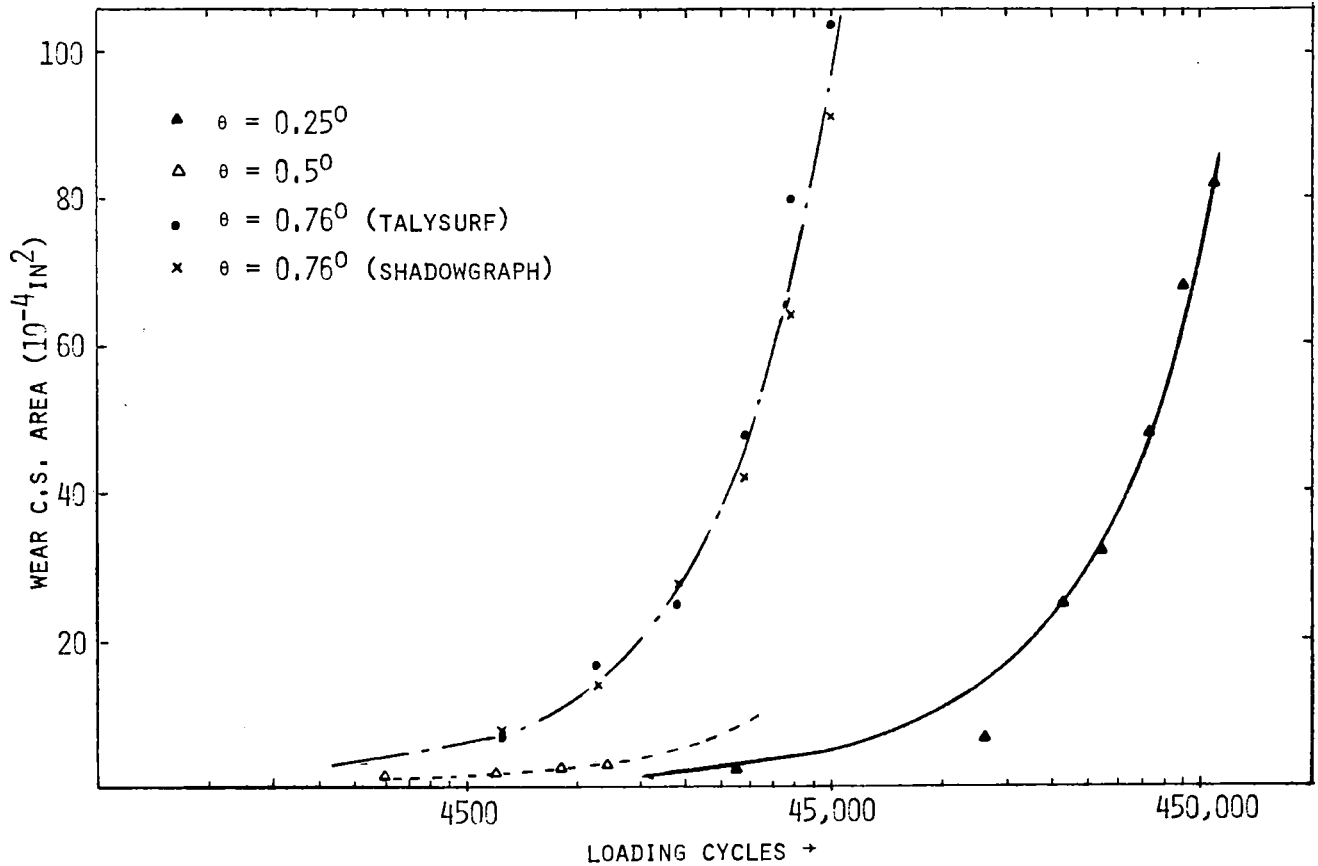


FIG. 9 TOTAL WHEEL WEAR CROSS SECTION AREA VS. CYCLES OF LOADING

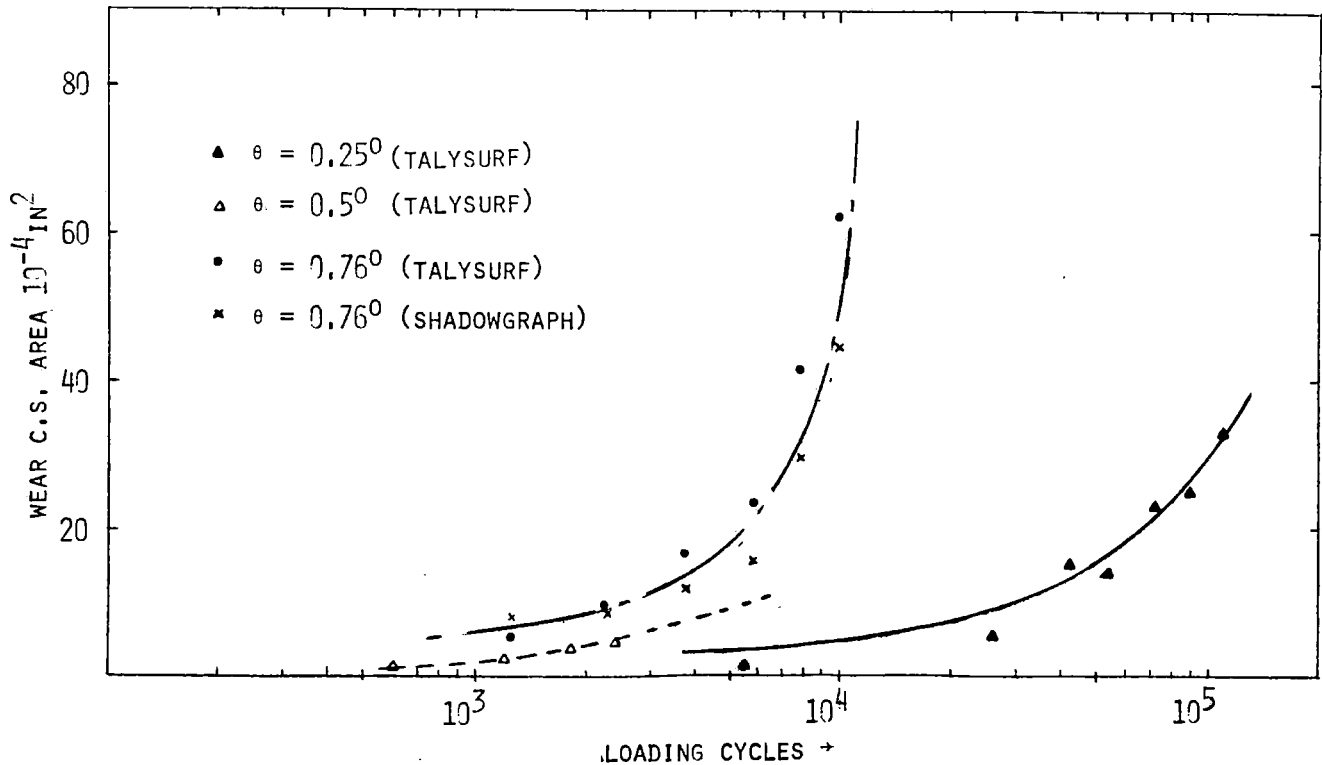


FIG. 10 TOTAL RAIL WEAR CROSS SECTION AREA VS. NO. OF CYCLES

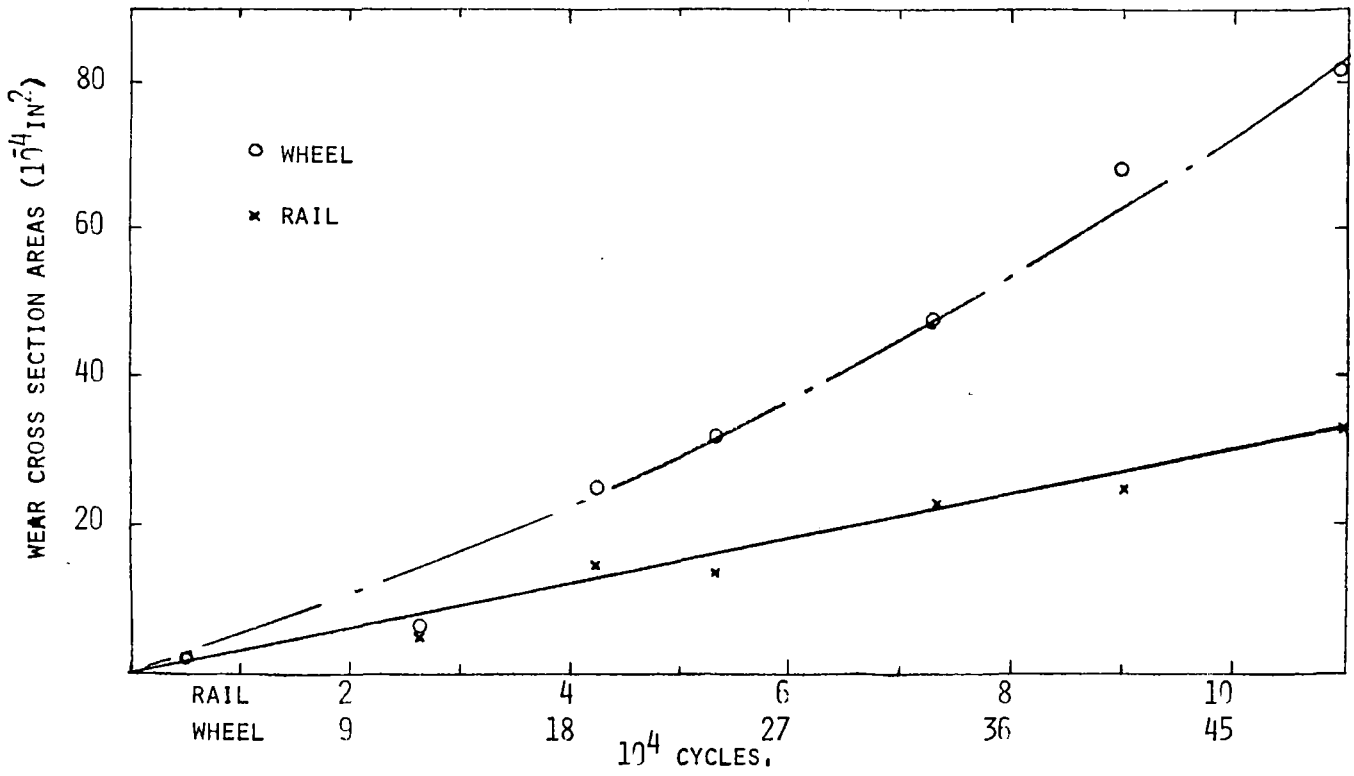


FIG. 11 TOTAL RAIL AND WHEEL WEAR C.S. AREAS VS CYCLES, $\theta = 0.25$ DEG.

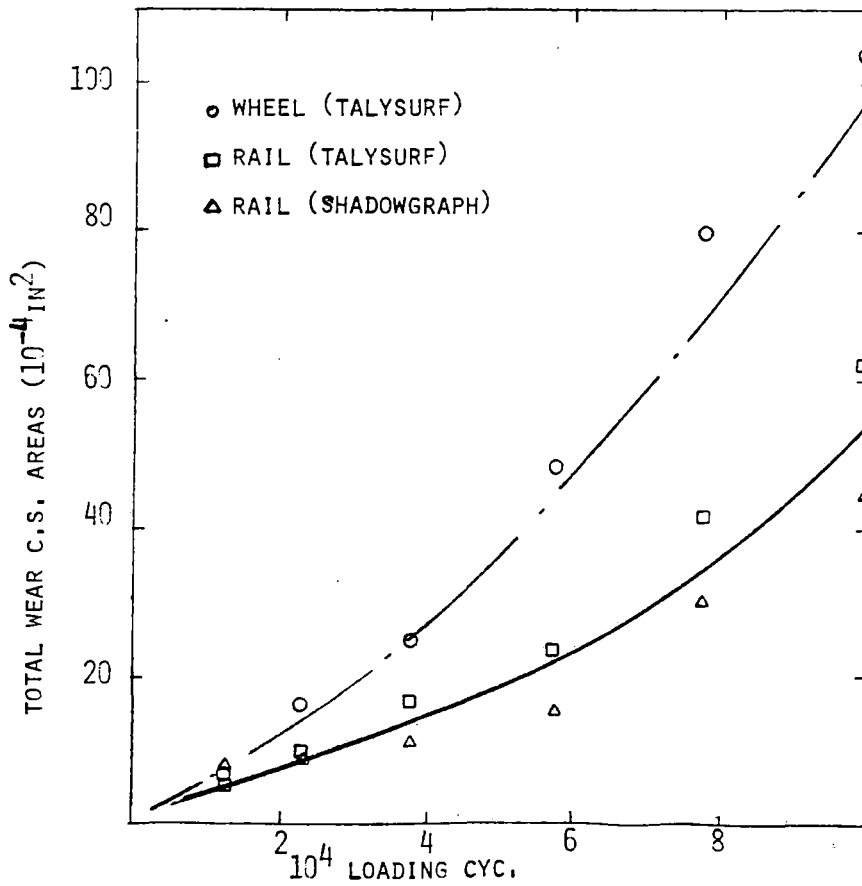


FIG. 12 TOTAL RAIL AND WHEEL WEAR C.S. AREAS VS CYCLES, $\theta = 0.76$ DEG.

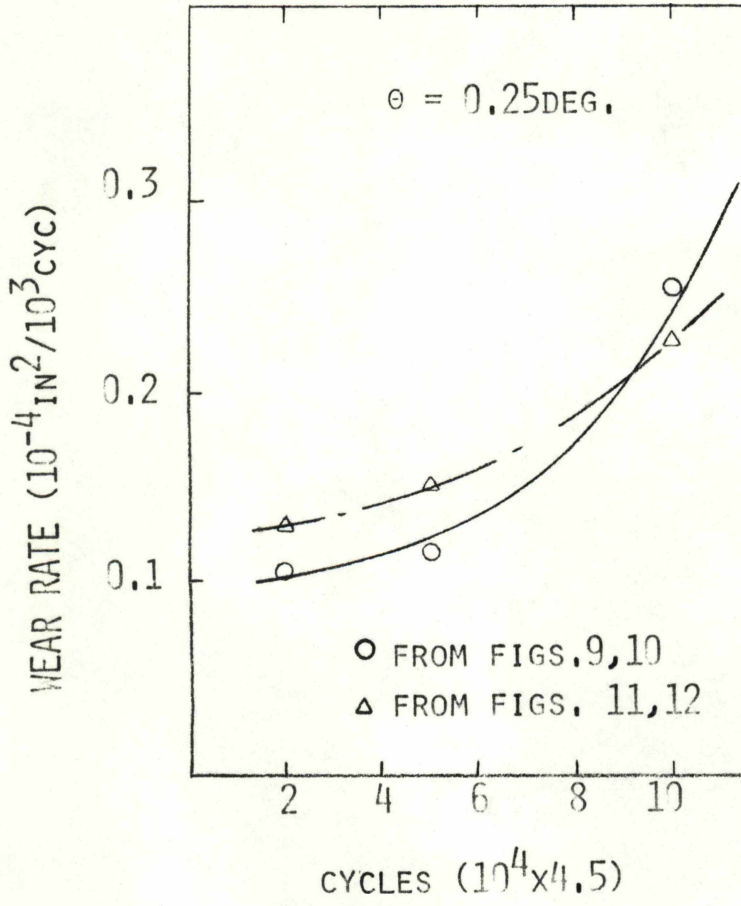
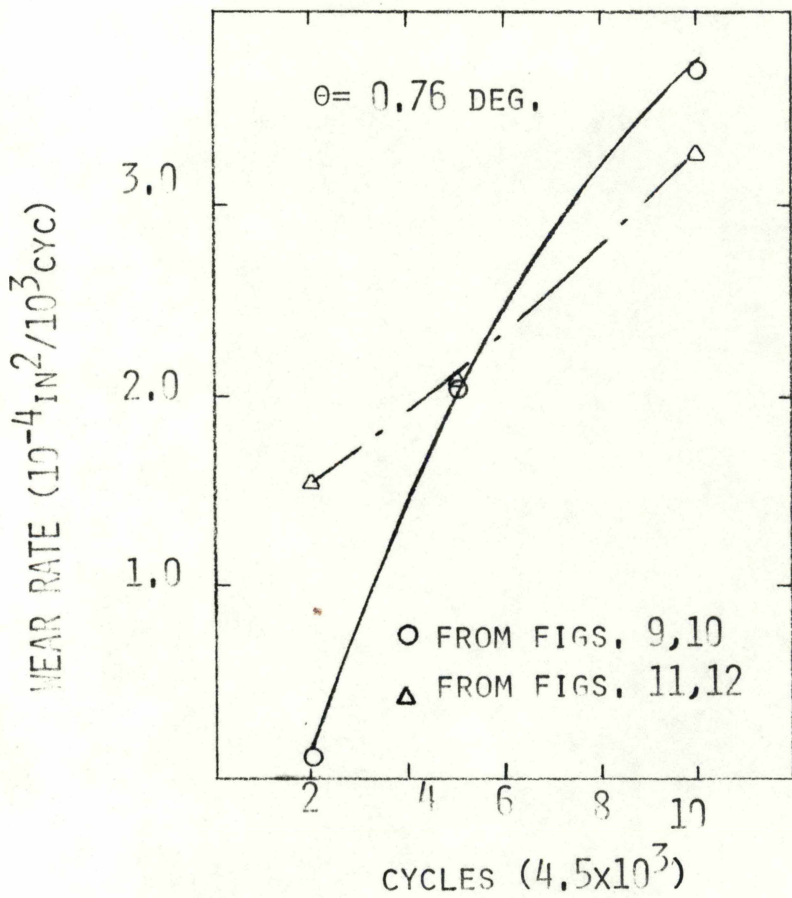


FIG. 13 WHEEL



WEAR RATE VS CYCLES OF LOADING.

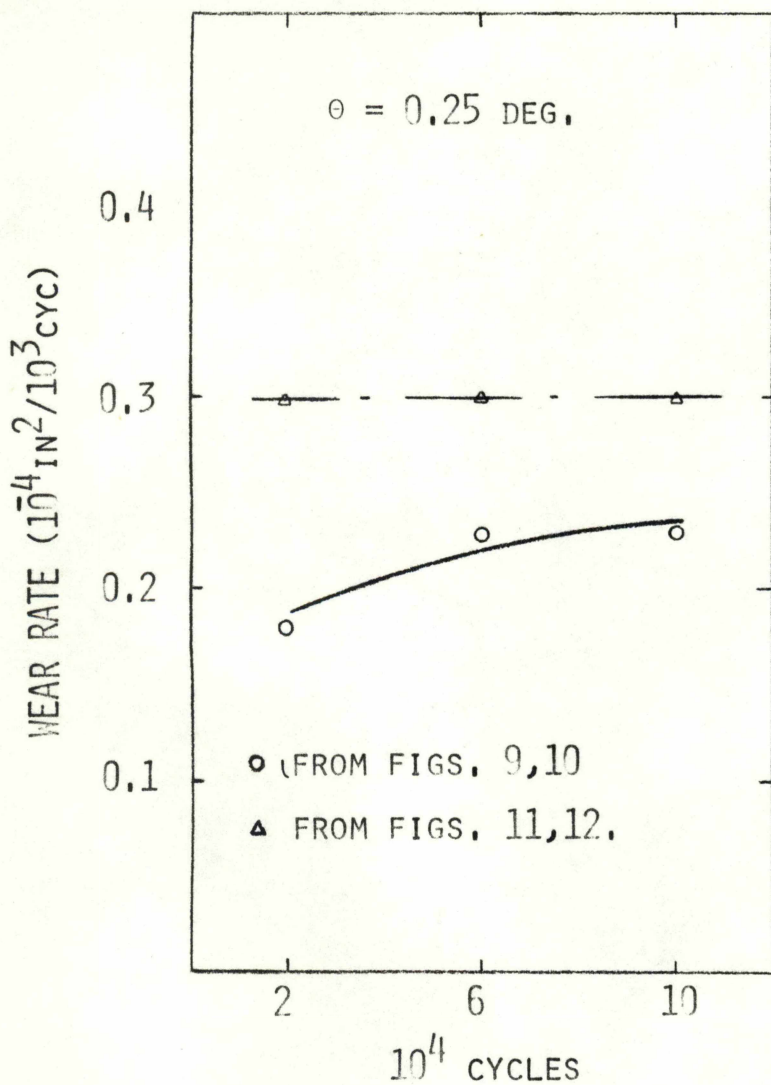
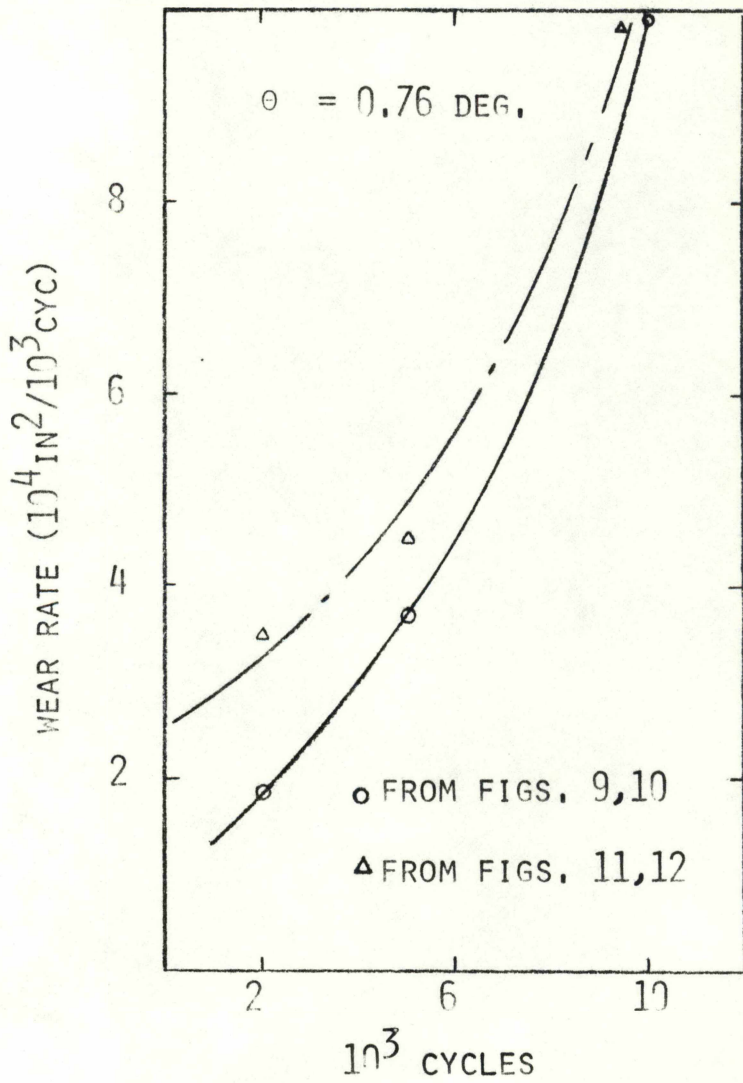


FIG. 14 RAIL WEAR



R RATE VS LOADING CYCLES.

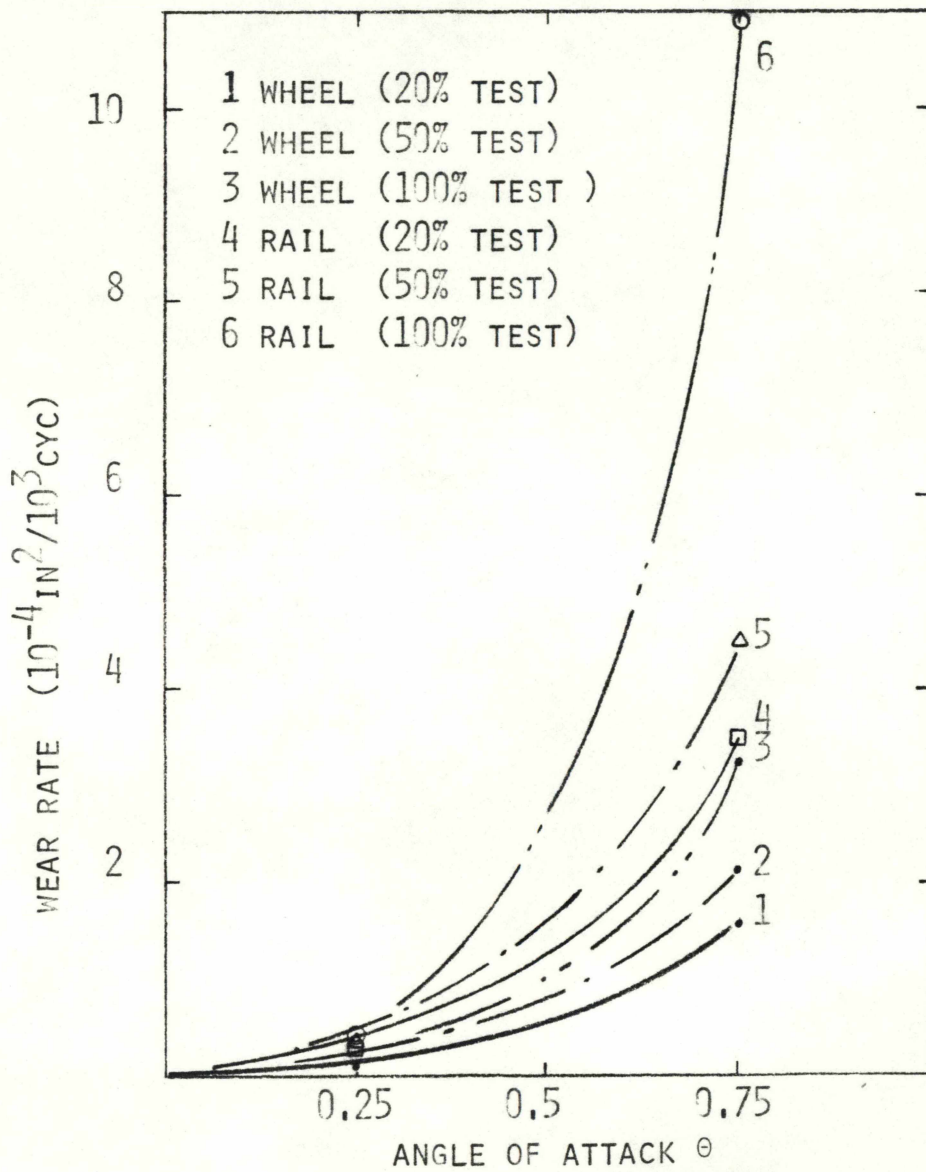


FIG. 15 WEAR RATE VS θ FOR WHEEL AND RAIL.

TABLE 7

Wear rates based on Figs. 9, 10, 11 and 12 ($10^{-4} \text{ in}^2 / 10^3 \text{ cycles}$)

| 1 Based on Figs. 9 and 10, 2 Based on Figs. 11 and 12 | | | | | | | | | |
|---|------|------|-------|------|-----------------------------------|-------|------|-------|------|
| <u>$\theta = 0.25$</u> | | | | | <u>$\theta = 0.76$</u> | | | | |
| | RAIL | | WHEEL | | | RAIL | | WHEEL | |
| CYCLES | 1 | 2 | 1 | 2 | CYCLES | 1 | 2 | 1 | 2 |
| 20,000 | 0.18 | 0.30 | 0.11 | 0.13 | 2000 | 1.84 | 3.5 | 0.11 | 1.56 |
| 50,000 | 0.23 | 0.30 | 0.11 | 0.15 | 5000 | 3.68 | 4.5 | 2.05 | 2.11 |
| 100,000 | 0.23 | 0.30 | 0.25 | 0.23 | 10,000 | 10.00 | 11.0 | 3.69 | 3.28 |

TABLE 8

Total wear volumes of wheel and rail

| <u>CYCLES</u> | Total wear volume (10^{-2}in^3) | |
|-----------------------------------|--|--------------|
| | <u>RAIL</u> | <u>WHEEL</u> |
| <u>$\theta = 0.25$</u> | | |
| 5500 | 1.92 | 0.65 |
| 12,500 | - | - |
| 26,000 | 6.22 | 1.66 |
| 42,500 | 17.19 | 6.18 |
| 53,500 | - | 7.99 |
| 73,000 | 26.12 | 12.04 |
| 90,000 | 28.16 | 17.04 |
| 111,000 | 37.09 | 20.61 |
| <u>$\theta = 0.76$</u> | | |
| 1250 | 6.33 | 1.72 |
| 2250 | 11.09 | 4.21 |
| 3750 | 19.23 | 6.31 |
| 5750 | 27.31 | 12.23 |
| 7750 | 47.39 | 20.07 |
| 10,000 | 70.46 | 26.20 |

log plots covering a large test range, whereas Figs. 11 and 12 are linear. The semi-log plot provides a possible comparison of wear at corresponding cycles in different tests.

The discussion up to this point has been in terms of wear cross sectional areas which show higher total wear of the wheel during a test compared to total rail wear. However, when wear volume is considered, one can see that more material is being removed from the rail in view of the large diameter of the laboratory wheel simulating the field rail. The wear volumes are tabulated in Table 8.

5. FLANGE WEAR INDICES AND FLANGE WEAR RATES

The flange wear indices to be checked out against the experimental wear rates are

$$a) \quad W_1 = \mu_f F_f \theta \quad [\text{Friction center method}] \quad (1)$$

where W_1 = Flange wear index

μ_f = Flange adhesion coefficient

F_f = Flange force

θ = Angle of attack (rad)

$$b) \quad W_2 = \mu_f F_f \left[\left(\frac{a}{r} \right)^2 + (\theta \tan \beta)^2 \right]^{1/2} \quad [\text{CN}] \quad (2)$$

where W_2 = Flange wear index

μ_f = Flange friction coefficient

F_f = Flange force (lbs)

a = Vertical distance from flange contact point to the wheel tread (in)

r = Wheel radius (in)

θ = Angle of attack (rad)

β = Flange angle

$$c) \quad W_3 = K_1 \theta + K_2 C_{22} \theta^2 \quad \theta < 20' \quad (3a)$$

$$= K_3 \theta \quad \theta > 20' \quad (3b)$$

[GHONEM & KALOUSEK]

where K_1, K_2, K_3 = Constants

C_{22} = Lateral creep coefficient

θ = Angle of attack (minutes of arc)

a) Index W_1

Since the experiments were all conducted on dry clean surfaces we may assume that

μ_f = Longitudinal peak coefficient of adhesion for the crown/tread.

= 0.54 (From Fig. 2)

The flange force actually experienced is the sum of the force due to angle of attack or lateral creepage and the externally

applied lateral load, though it would appear that only external forces on the flange are considered in most of the reported work.

The flange force during the two tests (using data of Fig. 1) are:

| θ | ξ (%) | Force due to lateral creepage from Fig. 1 | Measured External lateral load (lbs) | Estimated Total flange force (lbs) |
|----------|-----------|---|--------------------------------------|------------------------------------|
| 0.25 | 0.436 | 520 | 130 | 650 |
| 0.5 | 0.873 | 670 | 85 | 755 |
| 0.76 | 1.33 | 690 | 172 (Av) | 862 |

The calculated indices are compared with the average flange wear rate during the tests.

| θ | W_1 | | Measured Ave Flange Wear Rate ($10^{-4} \text{ in}^2 / 10^3 \text{ cyc}$) |
|----------|----------------------|---------------------------------|--|
| | Based on Total Force | Based on External Lateral Force | |
| 0.25 | 1.53 | 0.31 | 0.117 |
| 0.5 | 3.56 | 0.40 | 0.335 |
| 0.76 | 6.17 | 1.23 | 2.20 |

From the above table and Fig. 16, it would appear that the index W_1 (based on total load) does not correlate with the wear rates, at least for the type of testing wherein the angle of attack is maintained constant during the entire test. Further, the index W_1 would at best refer to an overall average wear rate during a test, whereas the controlled tests reported here show varying wear rates during various stages of the test.

Another undesirable feature of the index is the fact that it tends to zero for $\theta = 0$ even though the external load on the flange may not be zero. If on the other hand one were to consider F_f to consist of only the externally applied lateral load on the wheel as is usually done, the effect of θ is not brought out. It may seem at first sight that there is reasonably good correlation between wear rate observed and the wear rate index W_1 calculated on the basis of external force only acting on the flange. This is purely a coincidence since the real force acting on the flange is considerably higher than the external load used in the calculations. Had we selected a different (higher) lateral external load, the data and index would not be expected to show this apparent correlation.

b) Index W_2

The values of a and β in the wear index equation (2) are

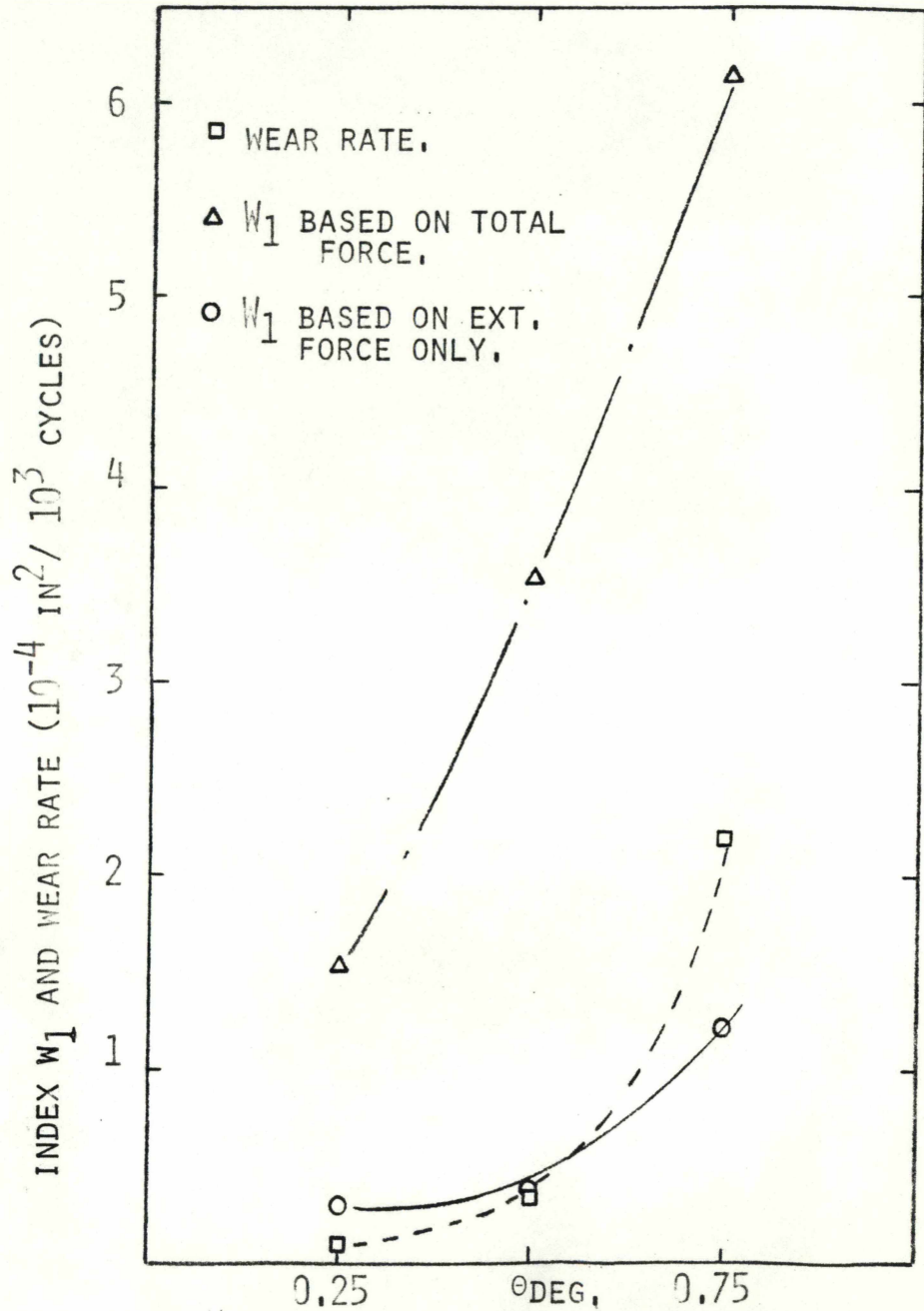


FIG. 16 W_1 AND FLANGE WEAR RATE VS θ

obtained by direct measurement from Figs. 7 and 8. For the purpose of estimating the distance "a" in the formula, flange contact point is assumed midway between tread and the extreme contact indicated on the worn profile. The flange angle β is estimated as the angle, to the horizontal, made by the tangent at the point of inflexion or tangent to the straight portion of the profile. The important parameters a and β could be accurately measured only for the $\theta = 0.76^\circ$ test. For this reason, this test was selected for checking out this index. The pertinent information is tabulated in Table 9.

The W_2 index indicates by simple inspection that for the typical values of the parameters observed in field, the second term is negligible. The index therefore reduces to

$$W_2 = \mu_f F_f \left(\frac{a}{r}\right)^2$$

for most cases. In this form, this index has no influence of β . If F_f is taken as only the lateral external force (which is often the case), this index has no influence of θ also. These are two major drawbacks of this index.

It so happens that, perhaps due to the right combination of values of the parameters used, the index shows an apparently moderate correlation with the wear rates as shown in Table 9.

However, if the index implied by Eq. 2 is the Marcotte, Caldwell, List index [5] given by

$$W_4 = \mu_f F_f \left[\left(\frac{a}{r}\right)^2 + (\theta \tan \beta)^2 \right]^{1/2} \quad (4)$$

the effects of θ and β are appreciable in relation to "a".

The Indices W_2 and W_4 as also the average wear rates during the test are tabulated in Table 10. A plot of these values is shown in Fig. 17. From the foregoing discussion and limited data, W_4 would appear to show a better agreement with the wear rate. However, the test data does not bring out the effect of θ . Unfortunately, the index could not be calculated for the 0.25° test.

c) Index W_3

The test data available at the present point of time is very limited. The average wear rates at various steady angles of attack are:

| θ | Flange Wear Rate ($10^{-4}/\text{in}^2/10^3 \text{ cyc}$) |
|----------|---|
| 0.25 | 0.18 |
| 0.50 | 0.34 |
| 0.76 | 2.20 |
| 1.00 | 6.10 |

TABLE 9

$$\theta = 0.76^\circ$$

$$W_2 = \text{Wear Index} = \mu_f F_f \left(\frac{a}{r}\right)^2 + (\theta \tan \beta)^2 \quad \mu_f = 0.54 \quad F_f = 862 \text{ lbs.} \quad r = 4.015$$

Flange wear rate in $10^{-4} \text{ in}^2 / 10^3 \text{ cycles}$

| Cycles | <u>a</u> | <u>β°</u> | <u>W_2</u> | <u>W_2 (Av)</u> | <u>Wear Rate (Av)</u> |
|--------|----------|---------------------------------|-------------------------|------------------------------|-----------------------|
| 0 | 1.25 | 64 | 45.11 | 60.68 | 1.52 |
| 2250 | 1.625 | 73 | 76.25 | 88.02 | 1.67 |
| 3750 | 1.859 | 79 | 99.79 | 108.57 | 2.06 |
| 5750 | 2.016 | 79 | 117.35 | 123.38 | 2.97 |
| 7750 | 2.117 | 80 | 129.41 | 136.76 | 2.55 |
| 10,000 | 2.234 | 80 | 144.11 | | |

TABLE 10

Comparison of W_2 , W_4 and wear rate

(Test data same as in Table 9)

| Cycles | <u>W_2</u> | <u>W_4</u> | <u>W_2 (Av)</u> | <u>W_4 (Av)</u> | <u>Av Wear Rate</u> ($10^{-4} \text{ in}^2 / 10^3 \text{ cyc}$) |
|--------|-------------------------|-------------------------|------------------------------|------------------------------|--|
| 0 | 45.1 | 145.5 | 60.7 | 167.5 | 1.52 |
| 2250 | 76.3 | 189.5 | 88.0 | 203.7 | 1.67 |
| 3750 | 99.8 | 217.9 | 108.6 | 226.9 | 2.06 |
| 5750 | 117.4 | 235.9 | 123.4 | 241.9 | 2.97 |
| 7750 | 129.4 | 247.9 | 136.8 | 254.7 | 2.55 |
| 10,000 | 144.1 | 261.4 | | | |

TABLE 10

Comparison of W_2 , W_4 and wear rate
(Test data same as in Table 9)

| <u>Cycles</u> | <u>W_2</u> | <u>W_4</u> | <u>W_2 (Av)</u> | <u>W_4 (Av)</u> | Av Wear Rate (10^{-4} in ² /10 ³ cyc) |
|---------------|-------------------------|-------------------------|------------------------------|------------------------------|---|
| 0 | 45.1 | 145.5 | 60.7 | 167.5 | 1.52 |
| 2250 | 76.3 | 189.5 | 88.0 | 203.7 | 1.67 |
| 3750 | 99.8 | 217.9 | 108.6 | 226.9 | 2.06 |
| 5750 | 117.4 | 235.9 | 123.4 | 241.9 | 2.97 |
| 7750 | 129.4 | 247.9 | 136.8 | 254.7 | 2.55 |
| 10,000 | 144.1 | 261.4 | | | |

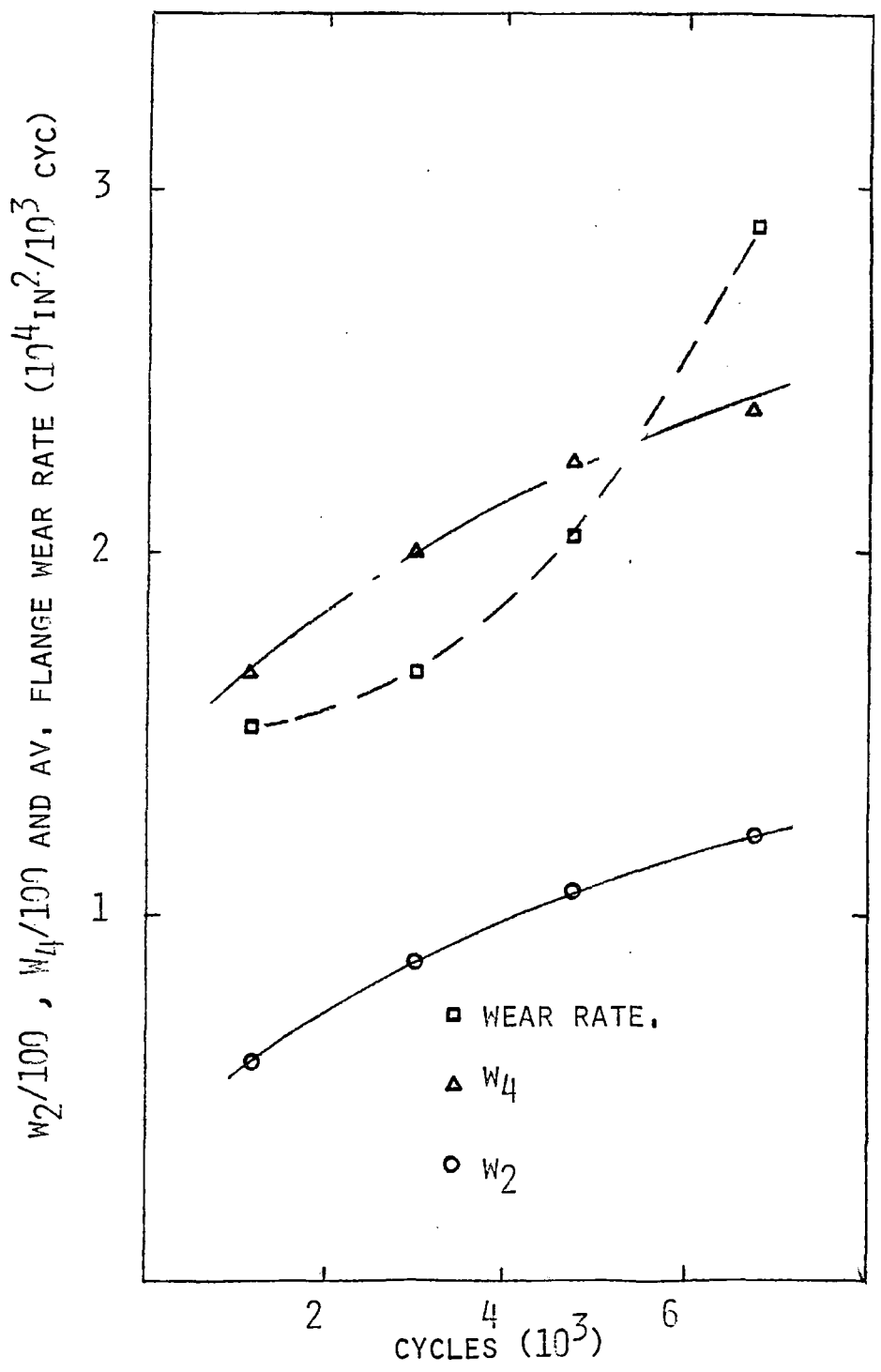


FIG. 17 W₂, W₄ AND FLANGE WEAR RATE VS CYCLES.

The flange wear rate does not show a linear dependence on θ as suggested by Eq. 3(b). For $\theta > 0.33^\circ$, in fact, the wear rate increase is more closely correlated by θ^2 in the range of tests conducted.

In the absence of the values of the various constants equations 3(a) and 3(b) cannot be checked out fully. However, an indirect method will be used which will permit a few more observations to be made about W_3 . For this purpose the life estimates suggested by Ghonem will be employed. The rail life $\gamma(\Psi)$ is given by

$$\gamma(\Psi) = (\Psi - 21.25)^2 + 148.45 \quad \Psi < 20' \quad (5a)$$

$$\gamma(\Psi) = 200 - 2.54 \Psi \quad \Psi > 20' \quad (5b)$$

Note Ψ is in minutes of arc

Defining $1/\gamma(\Psi)$ as $\gamma_1(\Psi)$ we can compare $\gamma_1(\Psi)$ with the experimentally established wear rates.

| θ | $\gamma_1(\Psi)$ [5a] | $\gamma_1(\Psi)$ [5b] | Observed Wear Rate |
|----------|-----------------------|-----------------------|--------------------|
| 0.25 | 0.0053 | 0.0062 | 0.18 |
| 0.50 | | 0.0081 | 0.34 |
| 0.76 | | 0.0119 | 2.20 |
| 1.00 | | 0.0210 | 6.10 |

It is seen that the wear rate does not correlate with the index. However, it should be pointed out that the experimentally established wear rates through the two experiments do not exhibit a tendency towards stabilization of the wear rate even though wear has progressed to quite a degree on both the rail and wheel. The wear rate increase beyond $\theta = 0.5^\circ$ is in fact not explained by the side force increase due to the increased angle. One observation in connection with the index W_1 is that it does not cater to the situations wherein an external lateral load, independent of the angle of attack, is present.

6. CONCLUDING REMARKS

- Angle of attack is an important parameter in wheel-rail contact studies. This is clear from a perusal of the μ - ξ relation wherein it can be seen that even small values of the angle of attack can be associated with large forces with the attendant consequences.
- The adhesion-creepage behavior of a wheel-rail pair exhibits the same basic qualitative features in the rolling (longitudinal) direction and the lateral directions.
- The adhesion-creepage relationship helps in establishing an accurate picture of the forces of interaction in the process of simulation of the rail-wheel interaction. In fact these are the forces which govern the observed phenomena of wear of the components.
- The wear of both wheel and rail are influenced quite strongly by the angle of attack. In fact increasing the angle of attack threefold, from 0.25° to 0.75° , reduces the life of the wheel by a factor of about 10.
- The wear rates mentioned show some variation, from experiment to experiment, influenced probably by small variations in the geometrical parameters.
- As the angle of attack is increased the flange wear gets to be a larger percentage of the total wear taking place. As evidenced by the 0.76° angle of attack test, at large angles of attack most of the wear taking place is in the flange area. This conclusion is however limited to the non-tractive conditions.
- Laboratory wear studies under constant angle of attack conditions represent a highly accelerated simulation of the same process in the field. Wear which takes place on a wheel in roughly 56×10^6 cycles is simulated by about 45,000 cycles at a steady 0.76° angle of attack. This is, of course, due to the fact that in the field, a wheel rarely, if ever, experiences an angle of attack of 0.76° in a steady fashion.
- None of the wear indices checked out in the present report show genuine correlation with the test data. Some shortcomings of the indices are quite evident by an inspection of the indices vis a vis the parameters they attempt to highlight. The limited data would indicate that the Marcotte, Caldwell, List index (W_4) shows some promise for use in the prediction process. However, the form of the index is quite complicated for ready application to field conditions.

- Study of the wheel-rail phenomena is a very complex process as brought out by the scatter of data obtained from closely controlled laboratory experiments. Limited experimental data available, as at present, is not adequate for firm conclusions of a quantitative nature to be drawn. Large number of experiments belonging to the family of geometrical simulation angle of attack trials are essential in order to generate precise numbers which can be used in the prediction process as an aid to design.
- It is to be recognized that the foregoing comments are offered for dry and clean interacting contacts of wheel and rail. The problem is more complex when such other factors as contamination, both intentional and unintentional, are considered.

7. RECOMMENDATIONS FOR FUTURE WORK

In the present study, only a few wear experiments could be conducted due to limitation of funds. These experiments show a certain trend of validity or non-validity of the wear indices. In order to have confidence in making such statements, a significant number of additional experimental investigations are necessary. These investigations should be conducted with appropriate geometrical simulations so that both flange and tread wear are included. The 8 important parameters that influence the wear of wheel and rail are vertical load V , lateral and vertical load ratio L/V , angle of attack θ , adhesion coefficient μ , hardness of the rail H_1 , hardness of the wheel H_2 , toughness of rail T_1 , and toughness of wheel T_2 . Kumar and Margasahayam [4] have conducted a dimensional analysis of wheel rail wear in which several important non-dimensional parameters have been determined. The additional experiments to be conducted should help evaluate and determine the influence of these important parameters. The following experiments should, therefore, be conducted:

- A. Single Metallurgy standard AAR rail and different metallurgy wheels. These experiments should utilize the presently available rail simulation and test wheels of different hardnesses including class U, class B and class C wheels. Experiments with class U should be conducted with 0.02 adhesion coefficient, whereas, with class B and C higher adhesion coefficient up to 0.5 should be developed. Several values of L/V ratios should be utilized from 0 to 0.75. Larger number of angle of attack between 0 and 1.5° should be used for a series of tests.
- B. Multiple metallurgy rails and different hardness wheels. Four sectors of rail of different metallurgies can be installed on the large wheel of the IIT facility. When installed a multiple metallurgy wear test can be conducted on this facility. It is important to conduct this investigation for determining the influence of increased hardness of the rail on wheel wear. At present there is a controversy regarding this influence. Controlled laboratory tests can help resolve this controversy.
- C. Material properties and wear relation investigation for wheel and rail steels. As indicated earlier, both the hardness and toughness of wheel and rail play an important role in the wear process. Two types of experiments should be conducted in order to determine this influence. Simple tension specimens made from rail and wheel steels should be tested to establish the toughness

and hardness characteristics of these steels. A second series of tests on a small roller rig should be conducted for determining rolling contact wear of these steels. The results of these 2 tests when combined can give an inter-relationship of hardness, toughness and wear.

- D. An attempt has been made at IIT to theoretically determine the various modelling parameters for wheel rail contact. These parameters should be utilized for a study of correlation of the laboratory data with wear data produced at F.A.S.T. Modifications of the modelling parameters should be conducted if necessary. As a result of the above analyses and experiments more refined measures of wear and degrees of validation of the currently available wear indices should be done. Such a study will enable a prediction and analysis of wheel and rail for the different railroad applications. An economic study of this process can then enable the railroads to decide on the most appropriate rails and wheels they should use for individual applications.

8. REFERENCES

1. Kumar, S., Rao, D.L. Prasanna, Rajkumar, B.R., "A Wheel Rail Wear Study for Railroad Transit Systems", IIT-TRANS-80-1, August 1980, report submitted to TSC, August 1980.
2. Kumar, S., Boulos, G.K., Shrimali, D., Rao, D.L. Prasanna, "Further Studies on Rail Wheel Wear", IIT-TRANS-80-3, November, 1980, p. 42, report submitted to AAR - Contract No. N-652.
3. Kumar, S., Chandrasekaran, K.S., Muhlenberg, J., "Design and Fabrication of a New Mechanism and Super Structure for the IIT-GMEMD Wheel Rail Simulation Facility", IIT-TRANS-80-2, report submitted to FRA - DOT-FR-744-4301, October, 1980.
4. Kumar, S., Margasahayam, R., "A Parametric and Experimental Analysis of Friction, Creep and Wear for Wheel and Rail on Tangent Track", Proc. ASME Symp. on the General Problem of Rolling Contact, 1980, AMD-Vol 40, pp. 139-155.

PROPERTY OF FRA
RESEARCH & DEVELOPMENT
LIBRARY

4390 Angle of Attack and Wheel-Rail Wear
02-Track-Train Dynamics